Structural Engineering and Mechanics, *Vol. 57, No. 1 (2016) 21-43*
DOI: http://dx.doi.org/10.12989/sem.2016.57.1.021

Identification of flexible vehicle parameters on bridge using particle filter method

S. Talukdar* and R. Lalthlamuana[a]

Department of Civil Engineering, Indian Institute of Technology Guwahati-781039, India

(Received February 12, 2014, Revised October 23, 2015, Accepted December 2, 2015)

Abstract. A conditional probability based approach known as Particle Filter Method (PFM) is a powerful tool for system parameter identification. In this paper, PFM has been applied to identify the vehicle parameters based on response statistics of the bridge. The flexibility of vehicle model has been considered in the formulation of bridge-vehicle interaction dynamics. The random unevenness of bridge has been idealized as non homogeneous random process in space. The simulated response has been contaminated with artificial noise to reflect the field condition. The performance of the identification system has been examined for various measurement location, vehicle velocity, bridge surface roughness factor, noise level and assumption of prior probability density. Identified vehicle parameters are found reasonably accurate and reconstructed interactive force time history with identified parameters closely matches with the simulated results. The study also reveals that crude assumption of prior probability density function does not end up with an incorrect estimate of parameters except requiring longer time for the iterative process to converge.

Keywords: conditional probability; vehicle flexibility; forward solution; bridge-vehicle interaction dynamics; noise level

1. Introduction

Moving vehicle imposes dynamic load on bridge pavement causing bridge to undergo vibrations. A comprehensive treatment of bridge-vehicle interaction dynamics and their practical application has been described by Fryba (1996), Yang *et al*. (2004). The estimation of dynamic load is significant in view of fatigue life estimation of both bridge and vehicle. Although, in majority of cases, dynamic load is marginally higher than static load but its action on bridge for several years causes continuous degradation of bridge and therefore, regular maintenance is necessary. It is difficult to measure interaction force between bridge and moving vehicle at a particular instant of time. Moreover, the weigh-in-motion system used by the regulatory body can measure only static axle load at slow motion and on smooth pavement. This condition is never achieved while vehicle moves on a bridge having various degrees of surface unevenness and speed variation. Therefore, it becomes a meaningful effort to find out the moving vehicle parameters using measured response of the bridge. Traditionally, instrumented vehicle (Mosses 1979, Clayton

*Corresponding author, Professor, E-mail: staluk@iitg.ernet.in
[a]Graduate Student, E-mail: r.lalth@iitg.ernet.in

http://www.techno-press.org/?journal=sem&subpage=8 ISSN: 1225-4568 (Print), 1598-6217 (Online)

and Peter 1990) or theoretical model of bridge-vehicle interaction (Green and Cebon 1997, Yang and Yau 1997) has been used to estimate the axle load and its effect on the pavement. Basically, the determination of vehicle parameters from bridge response measurement is an inverse problem. Research on the solution of such inverse problem has been started in identifying the static wheel load from measured bridge displacement or strain. A review paper on the recent status of works in this area has been published by Yu and Chan (2007). Connor and Chan (1988) have employed least square method to estimate equivalent static load and their dynamic variation with time based on bridge response measurement. Vehicle bridge interaction was ignored in the system model. An interpretive method has been developed by Law (1997) where bridge has been modeled as assembly of lumped masses and improvement of the model using Euler Bernouli continuous system has been considered by Chan *et al.* (1999). Laboratory experiments have been conducted by Chan *et al.* (2000) for identification of moving mass from measured strain. Later on, Law and Fang (2001) proposed a theoretical optimal state estimation with the use of dynamic programming, by which moving load could be identified, overcoming the difficulties of ill conditioning of state matrix in time and frequency domain approach encountered by the past authors (Law *et al*. 1997, 1999). Moving load identification in multi-span beams is also reported (Chan *et al.* 1999, Zhu and Law 2000) where effect of noise, number of vibration modes and effect of support flexibility for non rigid bearings has been considered. Development of Bayesian state estimation methodologies has added a new dimension in system identification involving various uncertainties (Kalman 1960). Most important Bayesian estimation is Kalman filtering which is applicable to linear models and Gaussian type of uncertainties. Ching *et al.* (2006), Nasrellah and Manohar (2010) applied a recently developed particle filter method for state as well as system parameter estimation of dynamic system. Many investigators commented particle filtering as a computationally expensive method although its efficiency has been admitted in reported application. To overcome the drawback of large computational time in a complex system, a relaxed Monte Carlo filter has been proposed by Sato and Tanaka (2013) by reducing number of particles in filtering stage. Yoshida and Akiyama (2013) developed a model updating process using particle filtering technique to monitor chloride induced damage of reinforced concrete structure in marine environment. Reports on moving load identification using particle filtering technique are scanty and therefore recognized as a new area of research in vehicle parameter identification from bridge response data. Further, literature survey reveals that most of the works on identification of moving load on bridge have considered vehicle model as rigid body. However, in recent years, long and slender multiaxle vehicles are frequently plying over the bridges carrying construction materials and other pay loads. This type of vehicle exhibits flexible modes under the influence of road excitation in addition to rigid body modes. The dynamic interaction of bridge with flexible vehicle and its application to solve inverse problems has not been addressed in the literature, although its necessity is being felt in modern days. In the present paper, Particle Filter Method (PFM) has been applied to estimate the vehicle parameters including its flexural rigidity. In addition the suspension and wheel characteristics are obtained using simulated bridge response. The identified vehicle parameters has been used to reconstruct interaction force time history and compared with the true value. The coupled bridge-vehicle dynamics in presence of non homogeneous random roughness of the bridge deck has been considered. The identification technique used in the paper has been examined in presence of noise with the response signal from different location along the span. Accuracy of the method with change in vehicle forward velocity and with various degrees of unevenness has been studied. The effect of range of the parameters to construct prior probability density function on the efficiency of the method has been discussed.

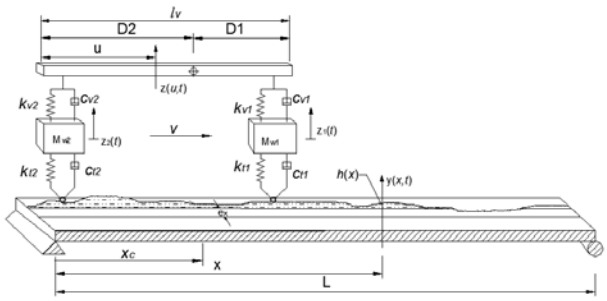

Fig. 1 Bridge-vehicle system model

2. Mathematical model

The bridge-vehicle model has been shown in Fig. 1. The bridge has been modeled as a uniform beam with simply supported end conditions. The mass, stiffness and damping are assumed to be uniform along the span of bridge. Due to eccentricity of the vehicle path, the bridge is subjected to flexure as well as torsion. The bridge deck is uneven which has been realized as non homogeneous process in spatial domain. This is represented by a function $h(x)$.

2.1 Equation of motion of vehicle

Vehicle body has been idealized as Euler-Bernoulli beam of length l_v. The behavior of suspension systems consisting of spring and dashpot are assumed as linear. The governing differential equation of motion of the vehicle deflection can be expressed as

$$E_v I_v \frac{\partial^4 z(u,t)}{\partial u^4} + C_v \frac{\partial z(u,t)}{\partial t} + m_v \frac{\partial^2 z(u,t)}{\partial t^2} = f_v(u,t) \tag{1}$$

in which m_v is the mass per unit length which includes self weight of the vehicle and payload. The symbols E_vI_v and C_v denote the flexural rigidity and viscous damping per unit length of the vehicle body, $z(u,t)$ represents vertical deflection of the vehicle body measured at location u from the reference point (taken at the left end of the vehicle) at time instant t. It may be noted that the heave-pitch model of vehicle known as 'Half Car model' has been adopted in the present study. The model facilitates the representation of multi-wheel and suspension at each axle location as single wheel and single suspension. This, in fact, replaces the multi-wheel input force at front or rear side of the vehicle as their resultant values. This type of vehicle model is widely accepted for bridge vehicle interaction studies (Wen 1960, Velestos and Huang 1970, Yang *et al*. 1999) and able to reflect vehicle bounce and pitching motion due to difference of wheel input caused by pavement unevenness. The impressed vertical force, now, can be written as

$$f_v(u,t) = \left[k_{v1}\{z(u,t) - z_1(t)\} + c_{v1}\{\dot{z}(u,t) - \dot{z}_1(t)\}\right]\delta(u-u_1) + \left[k_{v2}\{z(u,t) - z_2(t)\} + c_{v2}\{\dot{z}(u,t) - \dot{z}_2(t)\}\right]\delta(u-u_2) \tag{2}$$

where u_1 and u_2 represent the location of the attachment point of vehicle suspension from the reference point; z_1 and z_2 denote the vertical displacement of front and rear wheel masses respectively. k_{v1} and k_{v2} are the front and rear vehicle suspension stiffness respectively; c_{v1} and c_{v2} represent damping for vehicle front and rear suspension respectively. In Eq. (1) and (2), δ represents Dirac delta function with the property

$$\int_{-\infty}^{\infty} f(x)\delta(x-x_1)dx = f(x_1) \tag{3}$$

Nevertheless, the multi-axle inputs can also be considered in the present approach simply by adding more terms in Eq. (2) as the forces transmitted from other axle locations.

The equation of motion for the front un-sprung mass is given by

$$\begin{aligned} &m_1\ddot{z}(t)_1 + k_{t1}\{z_1(t) - y(x_1,t) - h(x_1)\} + k_{v1}\{z_1(t) - z(u_1,t)\} + c_{v1}\{\dot{z}_1(t) - \dot{z}(u_1,t)\} \\ &+ c_{t1}[\dot{z}_1(t) - \frac{D}{Dt}\{y(x_1,t) + h(x_1)\}] = 0 \end{aligned} \tag{4}$$

The equation of motion for the rear un-sprung mass is given by

$$\begin{aligned} &m_2\ddot{z}_2(t) + k_{t2}\{z_2(t) - y(x_2,t) - h(x_2)\} + k_{v2}\{z_2(t) - z(u_2,t)\} + c_{v2}\{\dot{z}_2(t) - \dot{z}(u_2,t)\} \\ &+ c_{t2}[\dot{z}_2(t) - \frac{D}{Dt}\{y(x_2,t) + h(x_2)\}] = 0 \end{aligned} \tag{5}$$

where, m_1 and m_2 are front and rear wheel mass respectively, k_{t1}, k_{t2} are front and rear suspension stiffness respectively; c_{t1}, c_{t2} are front and rear suspension damping respectively. $h(x_1)$ and $h(x_2)$ represents the non homogeneous deck profile under the front and rear wheels respectively. $y(x_1,t)$ and $y(x_2,t)$ are bridge displacements under front and rear wheels respectively at any instant of time t. $z(u_1,t)$ and $z(u_2,t)$ represents vehicle body deflection at the front and rear wheels position at any instant of time t. u_1 and u_2 is the location of wheel from the end of the vehicle body. Coriolis forces that arise due to rolling of wheel on the deflected profile of the bridge has been considered in the equation of motion using total derivative operator D/Dt (with $Dy/Dt=(\partial y/\partial x)\ (\partial x/\partial t)+\partial y/\partial t$). (Nasrellah and Manohar 2010, Fryba 1968).

2.2 Equation of motion of bridge

It is assumed that for symmetrical cross section (symmetrical about vertical axis), bending and torsion of the bridge would be independent under vertically applied live load. Thus governing differential equation of motion of the bridge in flexure can be expressed as

$$E_bI_b\frac{\partial^4 y(x,t)}{\partial x^4} + C_b\frac{\partial y(x,t)}{\partial t} + m_b\frac{\partial^2 y(x,t)}{\partial t^2} = f_b(x,t) \tag{6}$$

in which m_b, E_bI_b and C_b represents the mass per unit length, flexural rigidity and viscous damping per unit length of bridge. The impressed vertical force $f_b(x,t)$ on the bridge due to vehicle interaction is given by

$$\begin{aligned} f_b(x,t) = &-\left[k_{t1}\{z_1(t) - y(x,t) - h(x)\} + c_{t1}\left\{\dot{z}_1(t) - \frac{D}{Dt}[y(x,t) + h(x)]\right\}\right]\delta(x - x_1) \\ &-\left[k_{t2}\{z_2(t) - y(x,t) - h(x)\} + c_{t2}\left\{\dot{z}_2(t) - \frac{D}{Dt}[y(x,t) + h(x)]\right\}\right]\delta(x - x_2) \\ &-\{m_1 + \frac{1}{2}m_v l_v\} g\,\delta(x - x_1) - \{m_2 + \frac{1}{2}m_v l_v\} g\,\delta(x - x_2) \\ &+ m_1\frac{D^2}{Dt^2}[y(x,t) + h(x)]\delta(x - x_1) + m_2\frac{D^2}{Dt^2}[y(x,t) + h(x)]\delta(x - x_2) \end{aligned} \tag{7}$$

where g is the acceleration due to gravity. The governing differential equation of the bridge in torsion can be written as

$$G_b J_b \frac{\partial^2 \gamma(x,t)}{\partial x^2} - C_{bT} \frac{\partial \gamma(x,t)}{\partial t} - I_b \frac{\partial^2 \gamma(x,t)}{\partial t^2} = f_T(x,t) \tag{8}$$

in which I_b, G_bJ_b, C_{bT} and $\gamma(x,t)$ represents the mass moment of inertia per unit length, torsional rigidity, distributed viscous damping to rotational motion and torsional function of bridge. J_b is torsional constant, G_b is the shear modulus of beam material. $f_T(x,t)$ is the torque produced in the bridge cross section due to eccentric loading which is given by

$$\begin{aligned} f_T(x,t) = &-\left[k_{t1}\{z_1(t) - y(x,t) - h(x)\} + c_{t1}\left\{ \dot{z}_1(t) - \frac{D}{Dt}[y(x,t) + h(x)] \right\} \right] e_x \delta(x - x_1) \\ &-\left[k_{t2}\{z_2(t) - y(x,t) - h(x)\} + c_{t2}\left\{ \dot{z}_2(t) - \frac{D}{Dt}[y(x,t) + h(x)] \right\} \right] e_x \delta(x - x_2) \\ &- \{m_1 + \frac{1}{2} m_v l_v\} g\, e_x \delta(x - x_1) - \{m_2 + \frac{1}{2} m_v l_v\} g\, e_x \delta(x - x_2) \\ &+ m_2 \frac{D^2}{Dt^2}[y(x,t) + h(x)] e_x \delta(x - x_2)_x \delta(x - x_2) + m_1 \frac{D^2}{Dt^2}[y(x,t) + h(x)] e_x \delta(x - x_1) \end{aligned} \tag{9}$$

The parameter e_x in Eq. (9) denotes the eccentricity of vehicle wheels from the centre line of bridge deck.

2.3 Bridge deck roughness

In the present study we introduce a roughness, which is non homogeneous in space even though vehicle velocity is constant, by adopting following relation

$$h(x) = h_m(x) + \sum_{s=1}^{N} \varsigma_s \cos(2\pi \Omega_s x + \theta_s) \tag{10}$$

where $h_m(x)$ is a deterministic mean which represents construction defects, expansion joints, created pot holes, approach slab settlement, expansion joints, development of corrugation etc., ς_s is the amplitude of cosine wave, Ω_s is the spatial frequency (rad/m) within the interval [Ω_L Ω_U] in which power spectral density is defined. Ω_L and Ω_U are lower and upper cut off frequencies. The deck roughness is a Gaussian process (Shinozuka 1971) with a random phase angle θ_s uniformly distributed from 0 to 2π. N is the number of terms used to build up the road surface roughness. The parameters ς_s and Ω_s are computed as

$$\varsigma_s = \sqrt{2S(\Omega_s)\Delta\Omega}\ ;\ \Omega_s = \Omega_L + (s - 1/2)\Delta\Omega\ ;\ \Delta\Omega = (\Omega_U - \Omega_L)/N \tag{11}$$

in which $S(\Omega_s)$ is the power spectral density function (m^3/rad) taken from the reference (Huang and Wang 1992) modifying the same with addition of one term in denominator so that the function exists when $\Omega \rightarrow 0$.

$$S(\Omega_s) = S(\Omega_0) \times \frac{\Omega^2{}_0}{\Omega_s{}^2 + \Omega^2{}_L} \tag{12}$$

In the above equation, $\Omega_0 = 1/2\pi$ rad/m has been taken. The spatial frequency Ω (rad/m) and

temporal frequency ω (rad/s) for the surface profile is related with the vehicle speed V (m/s) as $\omega=\Omega_s V$. In the present study, vehicle forward velocity has been assumed constant.

2.4 Discretization of flexible vehicle equation of motion

As mentioned earlier vehicle body has been modeled as free-free beam which has two rigid modes and n_v number of elastic modes. It can be shown that when the translation of the mass centroid and the rotational motion about the mass centroid are considered, the two motions are orthogonal with respect to each other and with respect to the elastic modes (Hodges and Pierce, 2002). Thus total displacement of these rigid body degrees of freedom and elastic modes can be described by

$$z(u,t)=\sum_{j=-1}^{\infty}\phi_{vj}(u)\eta_j(t) \tag{13}$$

where $\phi_{vj}(u)$ is the vehicle mode shapes, the subscript v denotes vehicle, $\eta_j(t)$ is the time dependent generalized coordinate, j is the mode number; j=-1, 0 are taken to denote rigid body translatory and pitching mode, j=1,2,3…n_v represent elastic mode sequence of free-free beam and n_v is the number of significant flexible bending modes considered. The two rigid modes are vertical translation (heave) and rotation of longitudinal axis about centroid of the vehicle (pitc. The normalized rigid body translation can be represented by unity whereas rigid body rotation is to be represented by a liner function of distance from the trailing edge of the vehicle (Meirovitch 1967). The rigid body functions are taken as

$$\phi_{-1}=1;\quad \phi_0=u-D_2 \tag{14}$$

D_2 is a distance of vehicle centre of gravity from the trailing edge as given in Fig 1.

The elastic bending modes of free-free beam can be obtained by solving Eq. (1) in absence of external force. This is given by (Inman 2001)

$$\phi_{vj}=\sin(\alpha_j u)+\sinh(\alpha_j u)+\beta_j[\cos(\alpha_j u)+\cosh(\alpha_j u)];\quad \beta_j=\frac{\cos(\alpha_j l_v)+\cosh(\alpha_j l_v)}{\sin(\alpha_j l_v)+\sinh(\alpha_j l_v)} \tag{15}$$

The mode shape function for elastic bending given by Eq. (15) satisfies the zero shear and bending moment conditions at the free ends of the vehicle. The corresponding non dimensional frequency parameters $\alpha_j l_v$ can be related to circular natural frequency as

$$\omega_{vj}=\alpha_j^2\sqrt{\frac{E_v I_v}{m_v l^4{}_v}} \tag{16}$$

Substituting Eq. (13) in Eq. (1) and multiplying both sides of the equation by $\phi_{vk}(u)$ and then integrating with respect to u from 0 to l_v along with orthogonality conditions, the equation of motion can be discretized as

$$\ddot{\eta}_j(t)+2\xi_{vj}\omega_{vj}\dot{\eta}_j(t)+\omega_{vj}^2\eta_j(t)=Q_{vj}(t)\quad ;\ j=\text{-}1,0,1,2.... \tag{17}$$

Generalized force $Q_{vj}(t)$ in the j^{th} mode acting on the vehicle is given as

$$Q_{vj}(t) = \frac{1}{M_{vj}} \int_0^{l_v} f_v(u,t)\phi_j(u)du \tag{18}$$

in which generalized mass M_{vj} in the j^{th} mode is given by

$$M_{vj} = \int_0^{l_v} m_v \phi_{vj}^2(u)du \tag{19}$$

Making use of Eqs. (2) and (13) in Eq. (17) and integrating the expression using the property of Dirac delta function, one has the following expression for generalized force.

$$\begin{aligned} Q_{vj}(t) = \frac{1}{M_{vj}}[k_{v1}\{z_1(t) - \sum_{j=-1}^{n_v}\phi_j(u_1)\eta(t)\}\phi_j(u_1) + c_{v1}\{\dot{z}_1(t) - \sum_{j=-1}^{n_v}\phi_j(u_1)\dot{\eta}(t)\}\phi_j(u_1) \\ k_{v2}\{z_2(t) - \sum_{j=-1}^{n_v}\phi_j(u_2)\eta(t)\}\phi_j(u_2) + c_{v2}\{\dot{z}_2(t) - \sum_{j=-1}^{n_v}\phi_j(u_2)\dot{\eta}(t)\}\phi_j(u_2)] \end{aligned} \tag{20}$$

It may be mentioned that infinite number of modes are possible in continuous system considered in the present study. However, for practical implementation only first n_v modes of vehicle body has been included.

2.5 Discretization of bridge equation of motion

The bridge deflection in flexure be written as

$$y(x,t) = \sum_{k=1}^{\infty} \phi_{bk}(x) q_k(t) \tag{21}$$

where k=1,2,3...n_b; n_b represents number of significant bridge flexural modes. Subscript b represents bridge, $\phi_{bk}(x)$ is the flexural mode of the beam for simply supported boundary condition corresponding to natural frequency ω_{bk} and $q_k(t)$ are generalized co-ordinates in k^{th} mode (Inman 2001)

Now, substituting Eq. (21) in Eq. (6) and multiplying both sides of the equation by $\phi_{bj}(x)$ and then integrate with respect to x from 0 to L with the use of orthogonality conditions, the equation of motion can be discretized in normal co-ordinates as

$$\ddot{q}_k(t) + 2\xi_{bk}\omega_{bk}\dot{q}_k(t) + \omega_{bk}^2 q_k(t) = Q_{bk}(t) \quad ; k = 1,2,3...n_b \tag{22}$$

The generalized force $Q_{bk}(t)$ in the k^{th} mode of bridge in flexure is given as,

$$Q_{bk}(t) = \frac{1}{M_{bk}} \int_0^{L} f_b(x,t)\phi_{bk}(x)dx \tag{23}$$

in which generalized mass M_{bk} in the k^{th} mode is given by

$$M_{bk} = \int_0^{L} m_b \phi_{bk}^2(x)dx \tag{24}$$

The generalized force in the k^{th} of mode of bridge transverse vibration has been worked out as

$$
\begin{aligned}
Q_{bk}(t) = -\frac{1}{M_{bk}}\Bigg[& k_{t1}\left\{z_1(t) - \sum_{k=1}^{n_b}\phi_{bk}(x_1)q_k(t) - h(x_1)\right\}\phi_{bk}(x_1) + k_{t2}\left\{z_2(t) - \sum_{k=1}^{n_b}\phi_{bk}(x_2)q_k(t) - h(x_2)\right\}\phi_{bk}(x_2) \\
& + c_{t1}\left\{\dot{z}_1(t) - V\sum_{k=1}^{n_b}\phi'_{bk}(x_1)q_k(t) - V\sum_{k=1}^{n_b}\phi_{bk}(x_1)\dot{q}_k(t) - Vh'(x_1)\right\}\phi_{bk}(x_1) - \{m_1 + \frac{1}{2}m_v l_v\}g\phi_{bk}(x_1) \\
& + c_{t2}\left\{\dot{z}_2(t) - V\sum_{k=1}^{n_b}\phi'_{bk}(x_2)q_k(t) - V\sum_{k=1}^{n_b}\phi_{bk}(x_2)\dot{q}_k(t) - Vh'(x_2)\right\}\phi_{bk}(x_2) - \{m_2 + \frac{1}{2}m_v l_v\}g\phi_{bk}(x_2) \\
& + m_1\left\{\sum_{k=1}^{n_b}\phi_{bk}(x_1)\ddot{q}_k(t) + 2V\sum_{k=1}^{n_b}\phi'_{bk}(x_1)\dot{q}_k(t) + V^2\sum_{k=1}^{n_b}\phi''_{bk}(x_1)q_k(t) + 4Vh''(x_1)\right\}\phi_{bk}(x_1) \\
& + m_2\left\{\sum_{k=1}^{n_b}\phi_{bk}(x_2)\ddot{q}_k(t) + 2V\sum_{k=1}^{n_b}\phi'_{bk}(x_2)\dot{q}_k(t) + V^2\sum_{k=1}^{n_b}\phi''_{bk}(x_2)q_k(t) + 4Vh''(x_2)\right\}\phi_{bk}(x_2)\Bigg]
\end{aligned} \tag{25}
$$

in which (.) denotes time derivative. Repeating the similar steps, the discredited bridge equation for torsion in normal co-ordinate can be expressed as

$$\ddot{\gamma}_l(t) + 2\xi_{Tl}\omega_{Tl}\dot{\gamma}_l(t) + \omega_{Tl}^2\gamma_l(t) = Q_{Tl}(t);\ \ (l = 1,2,3...n_T) \tag{26}$$

Where n_T represents number of bridge torsional modes considered, ω_{Tl} and ξ_{Tl} are the natural frequency and modal damping coefficient of l^{th} mode in torsion respectively. The generalized torque in the l^{th} mode is given by

$$Q_{Tl}(t) = \frac{1}{M_{Tl}}\int_0^L f_T(x,t)\phi_{Tl}(x)dx \tag{27}$$

The torsional natural frequency ω_{Tl} and the corresponding mode Φ_{Tl} for the given simply supported boundary conditions for no warping restrains have been taken from reference (Inman, 2001). The generalized mass moment of inertia M_{Tl} in the l^{th} mode is given by

$$M_{Tl} = \int_0^L I_b\phi_{Tl}^2(x)dx \tag{28}$$

The generalized torque in the l^{th} mode can be expressed as,

$$
\begin{aligned}
Q_{Tl}(t) = -\frac{e_x}{M_{Tl}}\Bigg[& k_{t1}\left\{z_1(t) - \sum_{l=1}^{n_T}\phi_{Tl}(x_1)\gamma_l(t) - h(x_1)\right\}\phi_{Tl}(x_1) + k_{t2}\left\{z_2(t) - \sum_{l=1}^{n_T}\phi_{Tl}(x_2)\gamma_l(t) - h(x_2)\right\}\phi_{Tl}(x_2) \\
& + c_{t1}\left\{\dot{z}_1(t) - V\sum_{l=1}^{n_T}\phi'_{Tl}(x_1)\gamma_l(t) - V\sum_{l=1}^{n_T}\phi_{Tl}(x_1)\dot{\gamma}_l(t) - Vh'(x_1)\right\}\phi_{Tl}(x_1) - \{m_1 + \frac{1}{2}m_v l_v\}g\phi_{Tl}(x_1) \\
& + c_{t2}\left\{\dot{z}_2(t) - V\sum_{l=1}^{n_T}\phi'_{Tl}(x_2)\gamma_l(t) - V\sum_{l=1}^{n_T}\phi_{Tl}(x_2)\dot{\gamma}_l(t) - Vh'(x_2)\right\}\phi_{Tl}(x_2) - \{m_2 + \frac{1}{2}m_v l_v\}g\phi_{Tl}(x_2) \\
& + m_1\left\{\sum_{l=1}^{n_T}\phi_{Tl}(x_1)\ddot{\gamma}_l(t) + 2V\sum_{l=1}^{n_T}\phi'_{Tl}(x_1)\dot{\gamma}_l(t) + V^2\sum_{l=1}^{n_T}\phi''_{Tl}(x_1)\gamma_l(t) + 4Vh''(x_1)\right\}\phi_{Tl}(x_1) \\
& + m_2\left\{\sum_{l=1}^{n_T}\phi_{Tl}(x_2)\ddot{\gamma}_l(t) + 2V\sum_{l=1}^{n_T}\phi'_{Tk}(x_2)\dot{\gamma}_l(t) + V^2\sum_{k=1}^{n_T}\phi''_{Tk}(x_2)\gamma_l(t) + 4Vh''(x_2)\right\}\phi_{Tl}(x_2)\Bigg]
\end{aligned} \tag{29}
$$

2.6 Method of solution

The system of Eqs. (4), (5), (17), (22) and (26) are coupled second order ordinary differential equations. In general for continuous system like the ones (vehicle and bridge), presented in the

paper infinite number of modes exists. However, for practical applications, modes have to be truncated to a finite size. Let n_v, n_b and n_T be number of significant modes of vehicle motion, bridge flexural and torsional vibration respectively. The number of coupled equations becomes n=2+n_v+n_b+n_T. The system equations can be expressed in matrix notation as

$$[M]\{\ddot{r}(t)\}+[C]\{\dot{r}(t)\}+[K]\{r(t)\}=\{F(t)\} \tag{30}$$

where $\{r(t)\}=\{\eta_1(\mathrm{t}), \eta_1(t),\ldots,\eta_{nv}(t), z_1(t), z_2(t), q_1(t), q_2(t)\ldots,q_{nb}(t), \gamma_1(t), \gamma_2(t)\ldots, \gamma_{nT}(t)\}^T$ is the response vector, $\{F(t)\}$ is the generalized force vector and, $[M]$, $[C]$ and $[K]$ are system mass, damping and stiffness matrix respectively. Any direct integration method can be used to solve Eq. (30). In the present study, the Newmark-β method has been adopted (Bathe and Wilson 1987). Modal system response obtained from numerical integration is used to obtain bridge responses at various locations. The force vector $\{F(t)\}$ is a function of deck roughness and its derivative which are considered as a random process in the study. The response samples thus form complete ensemble of the process. Averaging across the ensemble at each time step yields mean $\mu_Y(\mathrm{t}_k)$ and standard deviation $\sigma_Y(t_k)$ of a response process Y.

3. Identification of vehicle parameters

Vehicle parameters estimation plays an important role in the axle load identification. This paper presents the applicability of PFM to identify the unknown vehicle parameters and estimate time dependent axle load on the bridge from the available bridge response measurements. The basic idea of PFM is to represent the required posterior density function of unknown vehicle parameters by a set of random samples (particles) with associated weights, and to compute the estimates based on these samples and weights. As the number of samples becomes very large, this Monte Carlo characterization becomes an equivalent representation of the posterior probability function, and the solution approaches the optimal Bayesian estimate.

Vehicle parameters to be identified include sprung and un-sprung masses, suspension stiffness damping, tyre stiffness and tyre damping which are represented by a vector $\{\Phi\}$. Bridge parameters and the velocity with which vehicle traverse the bridge is taken to be known. The system states r_l are assumed to propagate according to system equation

$$r_{l+1}=g_l(r_l,\eta_l)\ ; \qquad l=0,1,2,3\ldots. N_t \tag{31}$$

in which, l represents discretized time dimension and N_t is the number of time instants considered. $r_l \in R^n$ is a n-dimensional vector denoting the state of the system, a model noise $\eta_l \in R^m$ is the discretized m-dimensional vector of a sequence of independent and identically distributed random variables which are independent of past and current state and whose probability density function are assumed to be known. $g_l(.)$ is a system transition function. It is assumed that the transition function is such that $g_l(.) : R^n \times R^m \rightarrow R^n$.

When the system measurements become available, the system states are related to these measurements via the observation equation.

$$Z_l=f_l(r_l,\zeta_l)\ ;\ l=0,1,2,3\ldots. N_t \tag{32}$$

where $Z_l \in R^p$ is a p-dimensional bridge response measurement vector, a measurement noise $\zeta_l \in R^s$ is a s-dimensional vector of a sequence of independent and identically distributed random

variables and $f_l(.)$ is a non linear function that relates the measurements to the system state such that $f_l(.) : R^n \times R^s \rightarrow R^p$.

However, the main interest is on estimating the unknown vehicle parameters and that remains invariant with respect to time for the duration of measurements being taken. In writing the model equation, a model noise has to be added leading to the model equation as (Nasrellah and Manohar 2010)

$$\Phi_l = g_l(\Phi_{l-1}, \eta_l) \qquad l=0,1,2,3.... N_t \tag{33}$$

Here, as before, a model noise $\eta_l \in R^m$ is the discretized m-dimensional vector of a sequence of independent and identically distributed random variables with density $p(\Phi)$. It is further assumed that the initial conditions are random having a PDF $p(\Phi_0)$.

Similarly, the observation equation given in Eq. (32) can be written in terms of unknown vehicle parameters as

$$Z_l = f_l(\Phi_l, \zeta_l) \quad ; \qquad l=0,1,2,3.... N_t \tag{34}$$

Vehicle parameters identification problem can now be considered as being equivalent to the determination of the posterior probability density function $p(\Phi_l \mid Z_l)$. Thus knowing posterior PDF, also known as filtering density, one can determine the first few moments of the vehicle parameters Φ_l, conditioned on bridge response measurement $\mathbf{Z}_l$, at each time step. Mathematically, one can express first two moments as

$$\mu_{l|l} = \int \Phi_l p(\Phi_l \mid Z_l) d\Phi_l \tag{35}$$

$$\sigma^2{}_{l|l} = \int (\Phi_l - \mu_{l|l})^T (\Phi_l - \mu_{l|l}) p(\Phi_l \mid Z_l) d\Phi_l \tag{36}$$

The main steps of the particle filtering algorithm for identifying vehicle parameters now can be stated in a sequential manner for implementation in computer program in MATLAB environment (Arulampalam *et. al* 1991).

(i) For l=0, simulate N_p samples for Φ_0 from the assumed PDF $p(\Phi_0)$.

(ii) For l=1, calculate the prior prediction for the state, in this case denoted by Φ_l^*, from the model equation.

(iii) Once the measurements at the l^{th} state are available, the likelihood corresponding to all the samples $\{\Phi_{lj}^*\}_{j=1}^{Np}$ needs to be evaluated. This implies that one has to evaluate $\{p(Z_l \mid \Phi_{lj}^*)\}_{j=1}^{Np}$

(iv) To evaluate the likelihood for the samples, one requires to solve the associated equations and evaluate $\{f_l(\Phi_{lj})\}_{j=1}^{Np}$.

(v) Now, for the l^{th} measurement, calculate the weighting function as

$$w_j = \frac{p(Z_l \mid \Phi_{lj}^*)}{\sum_{j=1}^{N_p} p(Z_l \mid \Phi_{lj}^*)} \tag{37}$$

(vi) The discrete mass probability function for the next iteration is defined as

$$P[\Phi_{lj} = \Phi_l^*] = w_j \tag{38}$$

(vii) From the discrete mass distribution function, a new set of N_p samples of Φ_l are generated. This constitutes the posterior estimates of Φ_l.

(viii) The mean of estimates are obtained by averaging across the ensemble, and is expressed as

$$\mu_{l|l} = \frac{1}{N_p}\sum_{j=1}^{N_p}\Phi_{lj} \tag{39}$$

(ix) The corresponding standard deviation of the estimate is calculated as

$$\sigma_{l|l} = \sqrt{\frac{1}{N_p - 1}\sum_{j=1}^{N_p}(\Phi_{lj} - \mu_{l|l})^T(\Phi_{lj} - \mu_{l|l})} \tag{40}$$

When standard deviation becomes very small (less than or equal to tolerance value set by the programmer), the value of parameters are taken to be converged to true mean value. Otherwise, the above steps are repeated by setting l=l+1. In this way, the filtering is carried out for the entire available time history of measurements.

4. Result and discussion

In this study, the applicability of particle filter method in identifying moving vehicle load and its parameters based on measured bridge dynamic response has been demonstrated. Since no physical experiments have been undertaken, the measured response samples have been synthetically generated using the present analytical expression with artificial noise added to it to mimic field data.

A RC slab-girder bridge of span (L) 20 m with three longitudinal girders along the span and three cross girders, one at mid span and two at supports are selected for the study. The lane width: 8.6 m, Deck Thickness: 200 mm, concrete characteristic strength 25 N/mm^2. The cross section of the bridge is shown in Fig. 3(a). A Finite Element (FE) model of bridge in SAP2000 commercial software is first developed using above details of the bridge so as to match the fundamental natural frequency and first modal damping ratio of the simply supported beam model of T-beam bridge. The sectional properties of FE model is then used in the present numerical scheme. These are mass (m_b): 11.15×10^3 kg/m, flexural rigidity (E_bI_b): 3.7×10^{10} N-m^2, torsional rigidity (G_bJ_b): 1.695×10^{10} N-m^2.

For modeling deck surface roughness, the values of spectral roughness coefficient (ς) have been taken as 2×10^{-6} to 18×10^{-6} m^2/(m/cycle) according to International Organization for Standardization specifications for the class of different road conditions (ISO 8606 1995). The lower and upper limits of the spatial frequencies of the road profile are taken as ω_L=0.01 cycle/m and ω_U=3 cycle/m. The cut-off spatial frequencies are chosen in view of the practical size of tyre. The forward problem is solved using the assumed data and numerical integration employed to generate bridge dynamic responses.

A long vehicle carrying heavy load often crossing the bridge has been chosen to illustrate the present approach. The standards of vehicle are different from the live load prescribed by bridge code. In the present study, we use a Vehicle type: TATA 3516C-EX as shown in Fig. 3(b). Following are the important physical parameters pertaining to vehicle: length (l_v): 12 m, flexural rigidity (E_vI_v): 5.3×10^6 N-m^2, mass per unit length (m_v): 1500 kg/m, front and rear wheel masses (m_{w1}=m_{w2}): 800 kg each, Suspension stiffness front and rear (k_{v1}=k_{v2}): 3.6×10^7 N/m, Suspension

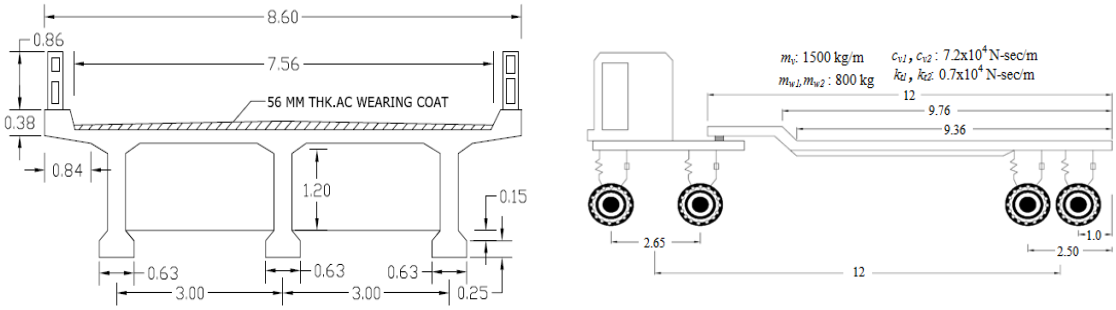

(a) Cross section of T-beam bridge (b) Vehicle model

Fig. 3 Cross section of bridge and vehicle model (All dimensions are in meter)

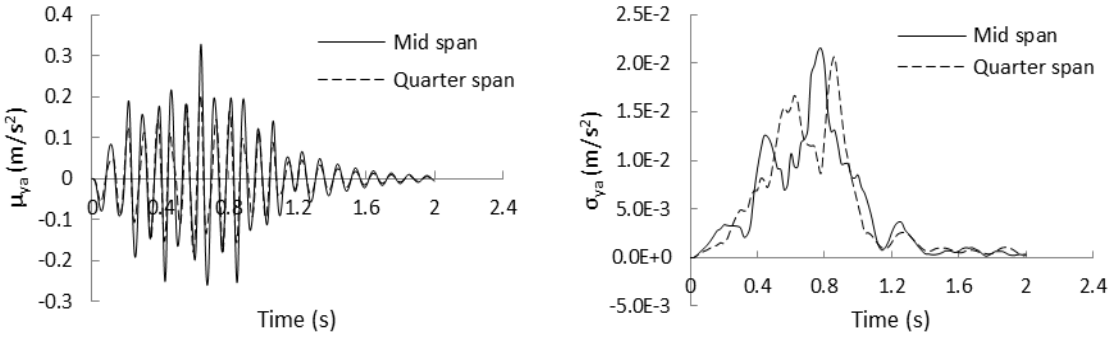

(a) Mean (b) Standard deviation

Fig. 4 Acceleration response of bridge at different location for constant vehicle speed 60 km/h

damping front and rear (c_{v1}=c_{v2}): 7.2×10^4 N-sec/m, front and rear tyre stiffness (k_{t1}=k_{t2}): 0.9×10^7 N/m, front and rear tyre damping (k_{t1}=k_{t2}): 0.7×10^4 N-sec/m. The representative vehicle in Fig. 3(b) has been idealized as heave-pitch (two inputs) model in the formulation. Therefore, tyre and suspension parameters of the vehicle adopted in numerical simulation represent the resultant values of two axle parameters located in front and rear side of the vehicle.

The main focus of the study is to find out the vehicle parameters from the measured dynamic response of the bridge using PFM. The mean acceleration time history at two stations (quarter and mid span) obtained by numerical solution was used. We first present the mean acceleration of the bridge at one fourth and middle span and corresponding standard deviation in Fig. 4(a) and Fig. 4(b) respectively. Vehicle velocity is taken as 60 km/h. No noise has been added at this stage. However, measured data will be considered in the particle filter algorithm by adding different level of noise. In the present study, two different level of noise 5% and 10% will be considered to test the convergence of filtering method. The mean quantities of mid span response is larger compared to other span locations. Standard deviation values do not show any definite pattern of variation.

4.1 Vehicle parameter identification

The PFM is now applied to estimate the unknown vehicle parameters which include vehicle mass, flexural rigidity, suspension stiffness, suspension damping, tyre mass, stiffness and damping.

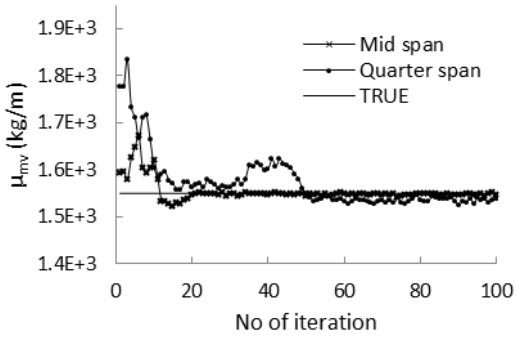

(a) Mean

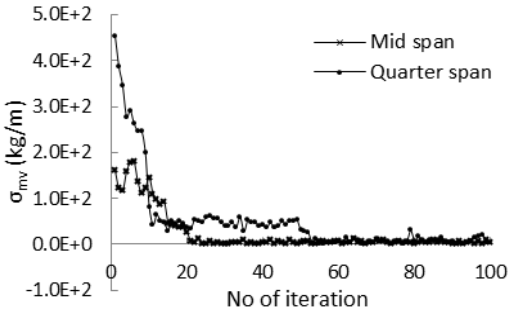

(b) Standard deviation

Fig. 5 Estimate of vehicle mass/length from acceleration data at different locations

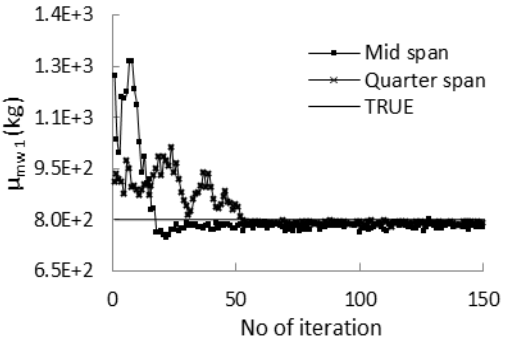

(a) Mean

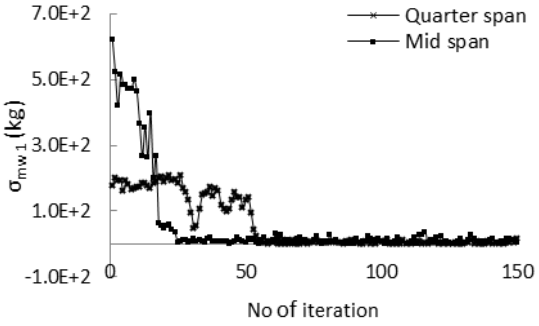

(b) Standard deviation

Fig. 6 Estimate of front wheel mass from acceleration data at different locations

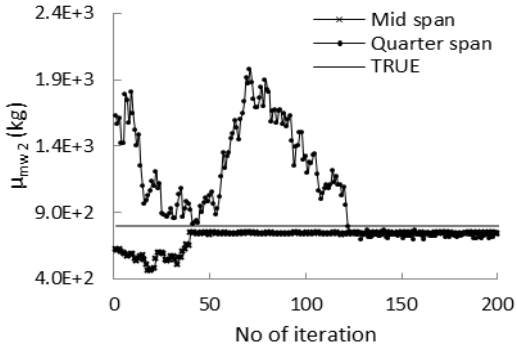

(a) Mean

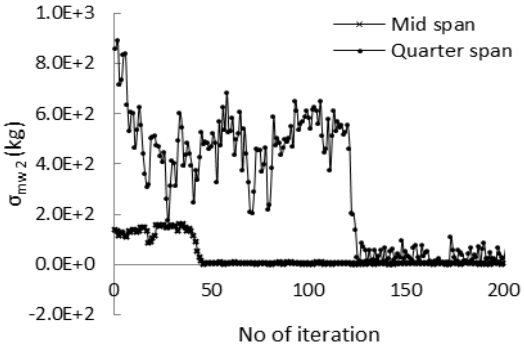

(b) Standard deviation

Fig. 7 Estimate of rear wheel mass from acceleration data at different locations

Only acceleration response of the bridge has been used as in most of the practical situation, acceleration response is picked up by the sensor. The numerically simulated bridge acceleration response has been contaminated by the addition of artificial noise to mimic field data. The iteration is started with a range of vehicle parameters which has been used to generate particles of assumed

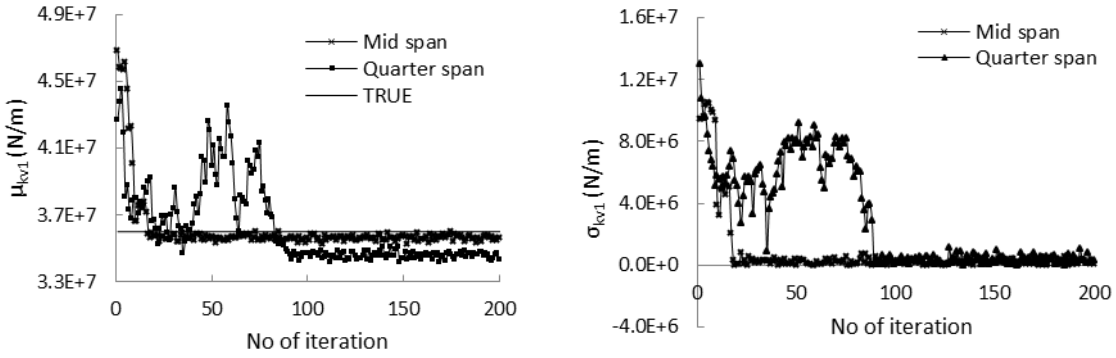

(a) Mean (b) Standard deviation

Fig. 8 Estimate of front suspension stiffness from acceleration data at different locations

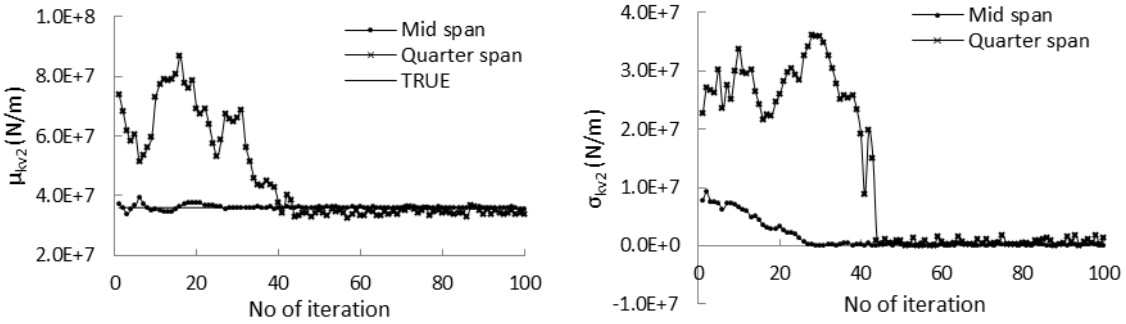

(a) Mean (b) Standard deviation

Fig. 9 Estimate of rear suspension stiffness from acceleration data at different locations

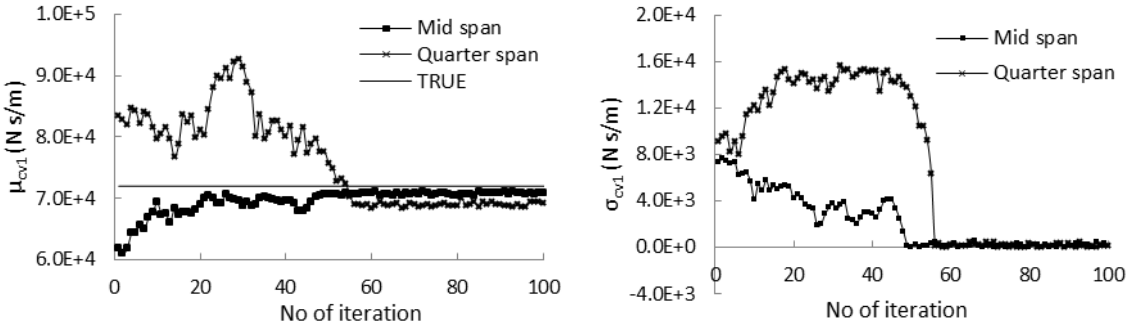

(a) Mean (b) Standard deviation

Fig. 10 Estimate of front suspension damping from acceleration data at different locations

probability density function. The mean and standard deviation values of the vehicle parameters are calculated at each stage of iteration at each time step of the synthetically generated time history. When the standard deviation of the parameters becomes very small, iteration is ended and observed as spike in the probability density curve. The progress of iteration and its convergence are presented in the subsequent sub sections taking various factors into considerations.

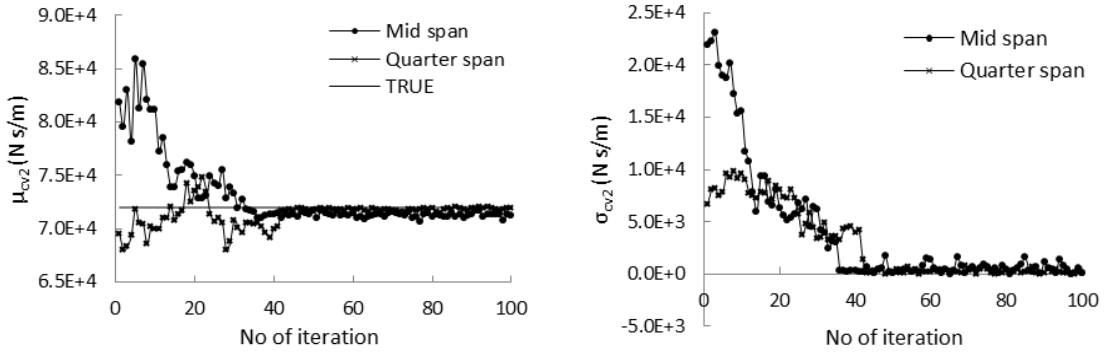

(a) Mean (b) Standard deviation

Fig. 11 Estimate of rear suspension damping from acceleration data at different locations

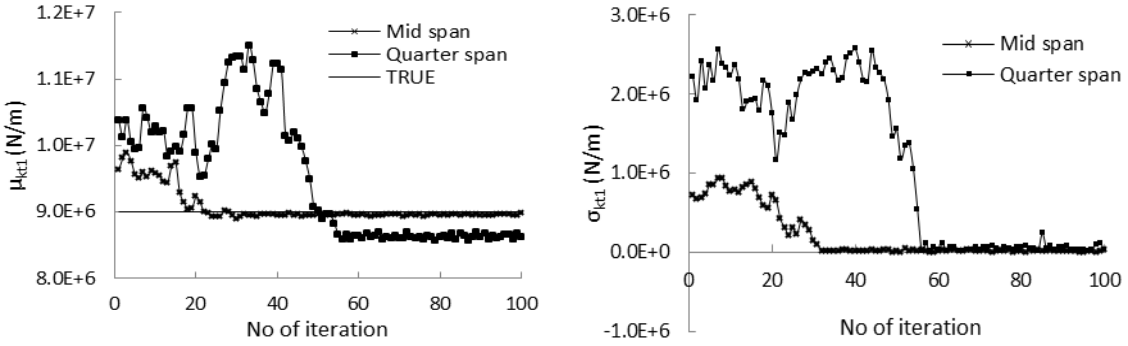

(a) Mean (b) Standard deviation

Fig. 12 Estimate of front tyre stiffness from acceleration data at different locations

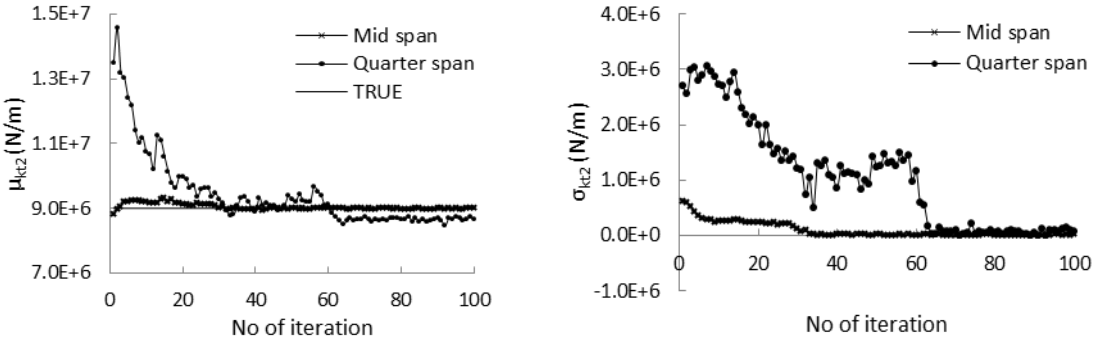

(a) Mean (b) Standard deviation

Fig. 13 Estimate of rear tyre stiffness from acceleration data at different locations

4.1.1 Effect of bridge response measurement location

The bridge acceleration measurement at different location along the span has been used as input to the particle filter algorithm. Having been estimated the vehicle parameters; the dynamic interaction force has been reconstructed and compared with the simulated value. The progress of

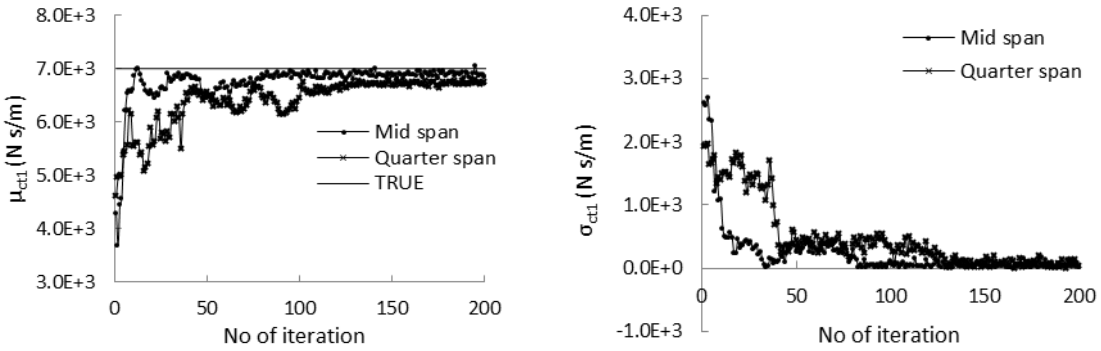

(a) Mean (b) Standard deviation

Fig. 14 Estimate of front tyre damping from acceleration data at different locations

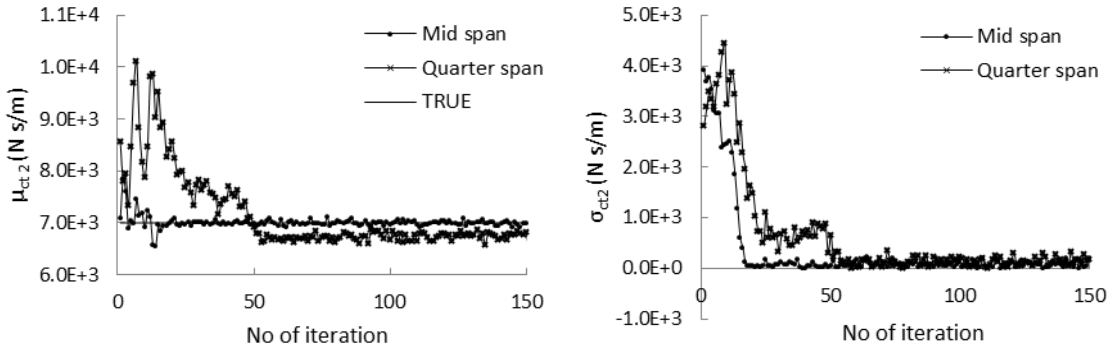

(a) Mean (b) Standard deviation

Fig. 15 Estimate of rear tyre damping from acceleration data at different locations

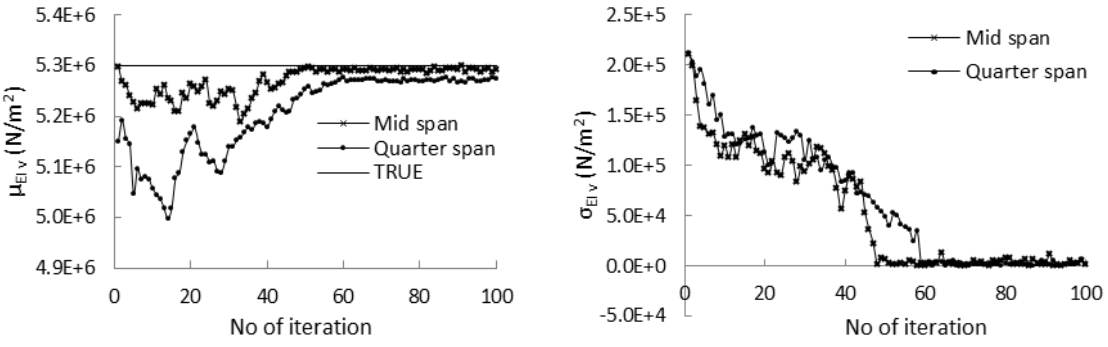

(a) Mean (b) Standard deviation

Fig. 16 Estimate of vehicle flexural rigidity from acceleration data at different locations

estimation of mean and standard deviation of some of the important vehicle parameters-mass/ length, flexural rigidity, wheel masses, suspension stiffness and damping has been displayed in the form of graphical plot of estimated parameters vs. corresponding number of iterations (Fig. 5 to Fig. 16).

Table 1 Effect of response measurement location on identified vehicle parameters

Parameters	No of iteration		Percentage error		Parameters	No of iteration		Percentage error	
	Mid span	Quarter span	Mid span	Quarter span		Mid span	Quarter span	Mid span	Quarter span
m_v	44	53	1.69	2.16	k_{t2}	33	60	5.016	9.37
k_{v1}	52	103	11.822	20.06	c_{t1}	49	102	14.49	20.96
k_{v2}	53	57	1.67	2.08	c_{t2}	58	61	1.667	3.64
c_{v1}	64	66	8.187	11.73	m_{w1}	45	64	8.76	8.96
c_{v2}	42	43	3.13	3.28	m_{w2}	28	115	2.343	7.37
k_{t1}	38	58	7.531	16.25	E_vI_v	48	59	1.085	2.53

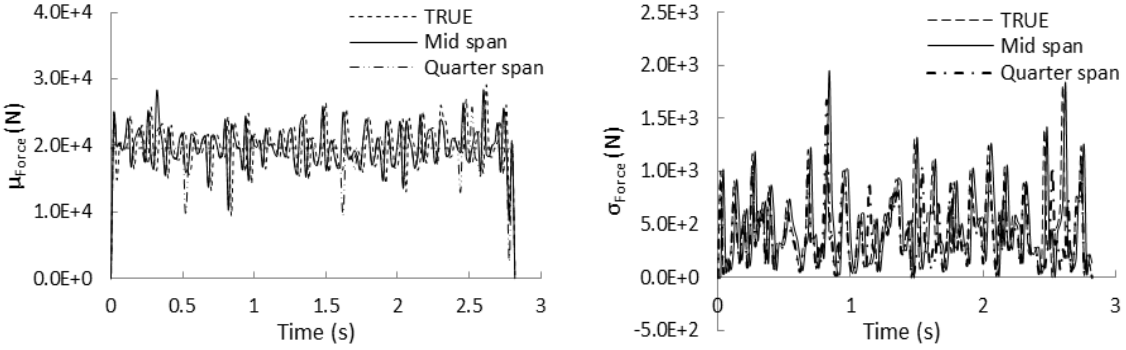

(a) Mean (b) Standard deviation

Fig. 17 Dynamic interaction force from different location of bridge acceleration response measurement

Table 1 presents number of iterations required for convergence and percentage deviation of identified parameters from true values using response samples at two different locations. The results show that estimate made from mid span response samples provide better accuracy compared to that of quarter span response samples used in present method. The mean and standard deviation of the vehicle-bridge interaction forces reconstructed from identified parameters have been shown in Fig. 17. It is seen that estimated dynamic force time history is close to the true value when mid span measurement or simulated samples are used in the algorithm. It is to be noted that number of iterations and percentage error differs in each parameter. It has been noticed that the sampling interval plays an important role for convergence and accuracy in the present numerical study. The simulation for the identification purpose in the present study has been carried out taking three sampling frequencies 300 Hz, 500 Hz and 700 Hz. Out of these, the results obtained using 500 Hz sampling frequency has been reported in the present paper. Use of higher sampling frequency, although, increases accuracy of estimate but has been found to delay the convergence. The similar observations has been reported by Law *et al.* (2004) while estimating moving load traversing on a beam using low sampling frequency. This could be due to the fact that high frequency component of random deck unevenness could not be properly filtered out with the low sampling frequency. However, the present results reflects that convergence has achieved after 28 to 48 iterations when mid span measurement is used. The number of iterations, however, remains in the higher range 43-115 when quarter span measurement is utilized. It may be noted

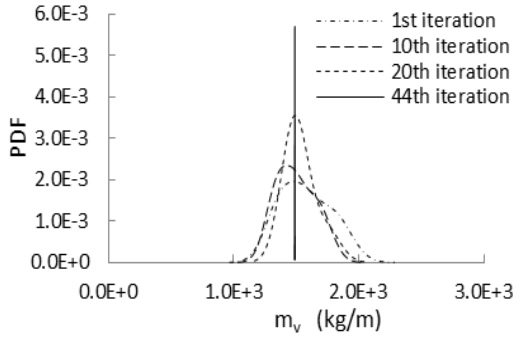

(a) Vehicle mass

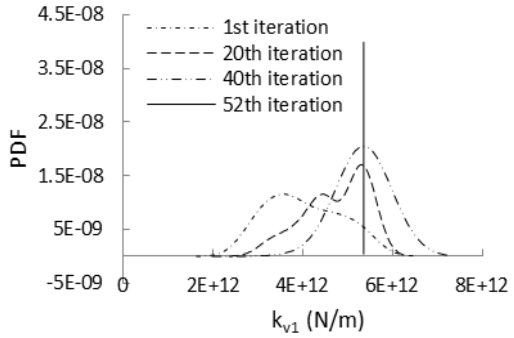

(b) Vehicle front suspension stiffness

Fig. 18 Evolution of Probability density function at different stages of iteration

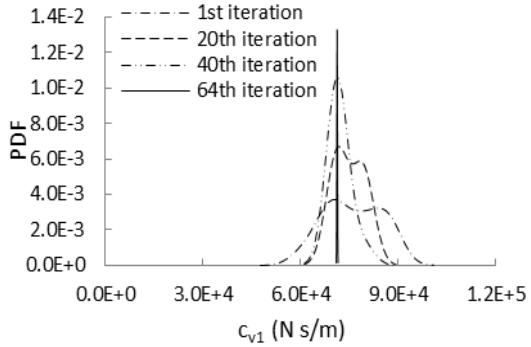

(a) Vehicle front suspension damping

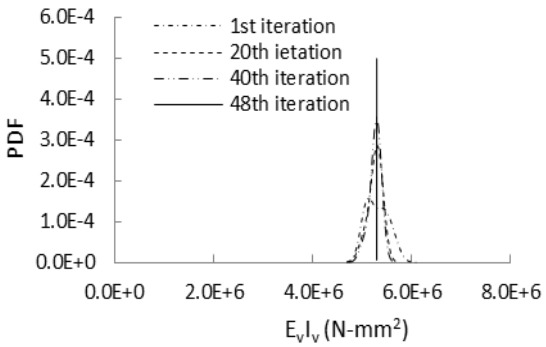

(b) Vehicle flexural rigidity

Fig. 19 Evolution of probability density function at different stages of iteration

that particle filtering method can accommodate model imperfection (Narsellah and Manohar 2013) in terms of added model noise which is necessary for the working of the method, and, thus, has rare possibility of failure to identify the hidden parameters.

It may be noted in Particle Filtering technique, probability density function of unknown parameters at each stage of iterations is updated until the convergence is achieved. The evolution of probability density function of some of the parameters to be estimated are shown at initial guess, at intermediate stages and at the end of identification process of some of the important parameters of the vehicle in Fig. 18 and Fig. 19. It may be mentioned that standard deviation approaches very low value at a certain number of iteration which implies that the algorithm has achieved convergence. A sharp peak of the probability mass function has been observed when convergence has been achieved. This is expected because of Gaussian excitation and linear system adopted in the study.

4.1.2 Effect of noise level

The effect of noise level on the algorithm has been tested by increasing it to 10%. Table 2 shows the percentage error as well as number of iteration required to converge, when noise level is increased. Result shows that, with the same accuracy more number of iterations is required when higher level of noise is added to the simulated bridge response. However, for some parameters it

Table 2 Effect of different noise level on the estimated vehicle parameters

Parameters	No of iteration		Percentage error		Parameters	No of iteration		Percentage error	
	5% noise	10% noise	5% noise	10% noise		5% noise	10% noise	5% noise	10% noise
m_v	44	51	1.69	1.67	k_{t2}	33	98	5.02	8.23
k_{v1}	52	69	11.822	13.44	c_{t1}	49	63	14.49	15.05
k_{v2}	53	48	1.67	4.95	c_{t2}	58	52	1.667	2.09
c_{v1}	64	59	8.187	15.95	m_{w1}	45	142	8.76	6.44
c_{v2}	42	47	3.13	1.26	m_{w2}	28	51	2.343	2.84
k_{t1}	38	63	7.531	10.01	E_vI_v	48	72	1.085	2.17

Table 3 Range of mass of vehicle, flexural rigidity and wheel mass to construct prior PDF

Range	Vehicle mass/length (m_v) kg/m		Vehicle flexural rigidity (E_vI_v) N-m^2		Front and rear wheel mass (m_{w1}, m_{w2}) kg	
	Case 1	Case 2	Case 1	Case 2	Case 1	Case 2
Γ_l	0.5×10^3	1.3×10^3	$1.5\text{x}10^6$	$5.8\text{x}10^6$	0.5×10^3	1.3×10^3
Γ_u	4.5×10^3	1.9×10^3	1.3×10^7	$1.1\text{x}10^7$	4.5×10^3	1.9×10^3

Table 4 Range of suspension stiffness, tyre stiffness, suspension damping and tyre damping to construct prior PDF

Range	Front and rear vehicle suspension stiffness (k_{v1}, k_{v2}) N/m		Front and rear wheel stiffness (k_{t1}, k_{t2}) N/m		Front and rear vehicle suspension damping (c_{v1}, c_{v2}) N-s/m	Front and rear wheel damping (c_{t1}, c_{t2}) N-s/m
	Case 1	Case 2	Case 1	Case 2	Case 1	Case 2
Γ_l	0.3×10^7	2.8×10^7	Γ_l	0.3×10^7	1.5×10^4	6.5×10^4
Γ_u	8.5×10^7	4.0×10^7	Γ_u	8.5×10^7	12.3×10^4	8.3×10^4

has been observed that faster end of iteration process even in presence of increased noise.

4.1.3 Effect of assumption of the prior PDF $p(\Gamma_0)$

In the absence of any information about the unknown parameters, it is assumed that the prior *PDF* $p(\Gamma_0)$ is uniformly distributed within a range $[\Gamma_l \quad \Gamma_u]$. Two different cases have been considered to specify the range within which random particles are generated assuming uniform probability density function $p(\Gamma_0)$. Case (i): Keeping the lower and the upper limits with large variation from the true value. Case (ii): Keeping the lower and upper limits close to the true value.

The range of values of the parameters assumed for the above two cases are mentioned in Tables 3 and 5. In these two cases, number of particles Np=1000 and artificial noise is taken to be 5% of the simulated maximum bridge dynamic response. The mean and standard deviation is observed at each stage of iteration and stopped when standard deviation becomes less than equal to tolerance.

It has been found that a incorrect choice of $p(\Gamma_0)$ does not necessarily lead to wrong estimates by the particle filter identification method. However, a crude assumption of the prior probability density is found to consume longer time to achieve convergence. Identified vehicle bridge interaction force is shown in Fig. 20 simultaneously comparing with the true value of dynamic

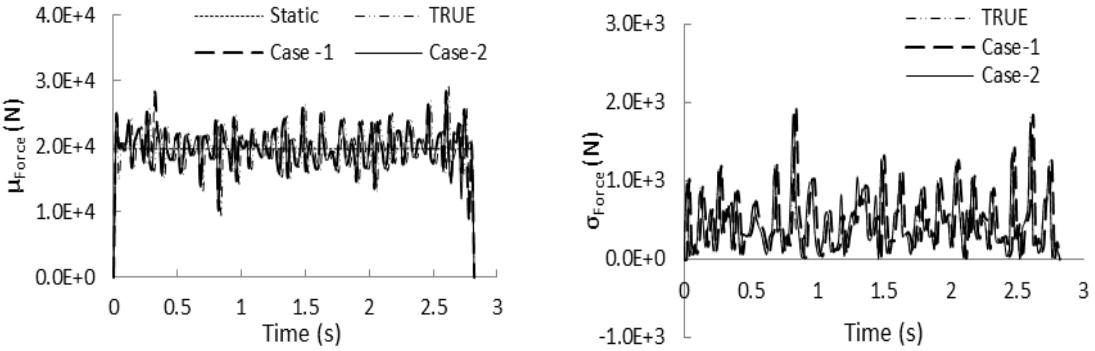

(a) Mean (b) Standard deviation

Fig. 20 Dynamic interaction force for different prior *PDF* $p(\Gamma_0)$

Table 6 Effect of vehicle speed on the estimated vehicle parameters

Parameters	No of iteration			Percentage error			Parameters	No of iteration			Percentage error		
	40 km/h	60 km/h	80 km/h	40 km/h	60 km/h	80 km/h		40 km/h	60 km/h	80 km/h	40 km/h	60 km/h	80 km/h
m_v	57	44	31	2.40	1.69	1.97	k_{t2}	62	33	106	1.90	5.02	6.67
k_{v1}	34	52	46	10.61	11.82	12.75	c_{t1}	56	49	32	11.73	14.49	15.60
k_{v2}	77	53	19	5.60	9.67	10.87	c_{t2}	81	58	93	2.07	1.67	4.59
c_{v1}	41	64	93	2.73	8.19	8.50	m_{w1}	21	45	63	1.23	8.76	7.58
c_{v2}	22	42	48	1.24	3.13	1.69	m_{w2}	18	28	65	1.78	7.14	9.41
k_{t1}	59	38	51	1.37	7.53	8.06	E_vI_v	26	48	94	2.18	3.09	3.43

interaction force. Assumption based on the first case of prior density function leads to 2 to 19 percent error while the second case assumption gives 1 to 14 percent error.

4.1.4 Effect of different vehicle velocity

The identification algorithm has been examined from the measured response for different vehicle speed over the bridge. The response samples have been generated at 40, 60, 80 km/h of vehicle speed. The sampling time interval in measured response sample (after adding 5% artificial noise) has to be chosen based on vehicle forward velocity so as to obtain sufficient data points. Number of iteration required to get convergence and resultant percentage error are tabulated in Table 6. It has been found that lower speed gives better estimate but it requires more number of iteration to achieve the convergence. Further, it has been observed that error in parameter estimation does not depend solely on the vehicle speed; rather there is necessity of adequate data points for satisfactory performance.

4.1.5 Effect of different roughness condition

Bridge deck surface irregularity has been considered in the identification of vehicle parameters based on ISO specification (ISO 8606:1995) for different conditions- good, average and poor. Among the three conditions, results show that good condition of pavement, gives the best estimate with less number of iteration as shown in Table 7. This may be attributed to the reason that noise

Table 7 Effect of vehicle speed on the estimated vehicle parameters

Parameters	No of iteration			Percentage error		
	Good condition	Average condition	Poor condition	Good condition	Average condition	Poor condition
m_v	24	44	47	1.30	1.69	2.21
k_{v1}	30	52	69	11.28	11.82	12.41
k_{v2}	19	53	49	3.95	9.67	7.11
c_{v1}	59	64	138	7.89	8.19	11.98
c_{v2}	38	42	92	2.13	3.13	8.70
k_{t1}	29	38	62	6.59	7.53	9.33
k_{t2}	31	33	55	3.28	5.02	11.83
c_{t1}	44	49	137	11.20	14.49	15.28
c_{t2}	47	58	110	2.86	1.67	4.55
m_{w1}	33	45	167	4.99	8.76	9.86
m_{w2}	23	28	127	3.79	7.14	8.55
E_vI_v	52	48	108	3.87	3.09	5.71

effect in dynamic input for the case of rougher pavement increases, requiring more number of iterations for convergence. This is in conformity with the results obtained when artificial noise level was increased from 5% to 10% in as stated earlier.

5. Conclusions

In the present study, Particle Filter method (PFM) has been employed for identification of vehicle parameters. Bridge parameters and vehicle speed were assumed to be known. However, PFM has general applicability in system identification and can also be used to identify bridge parameters which exist in coupled dynamic system. The efficiency of the proposed method has been studied by synthetic bridge acceleration response. The dynamic interaction force time history has been reconstructed with the identified parameters and compared with mean value. Different measurement location at the bridge span and effect of artificially added noise has been investigated. The accuracy of the proposed method has been checked by considering two different cases of prior density function selection. Some of the major findings and recommendations on the applicability of particle filter technique for vehicle parameter identification are given below:

• Response Measurement location has greater influence on the accuracy and computational time required in application of particle filtering technique. For simply supported single span bridge like the one being presented, mid span location of sensor point may be the better option.

• For identification of vehicle parameters with greater accuracy and within short time, response picked up at lower vehicle movement would be preferable for the implementation of particle filtering method.

• Rough bridge deck surface and presence of measurement noise would require more time for the convergence of the result.

• The initial wrong assumption of parameters of prior probability density function does not eventually lead to wrong estimate, except that the convergence time would increase.

References

Arulampalam, M.S., Maskel, S., Gordon, N. and Clapp, T. (2002), "A tutorial on particle filters for online nonlinear/non_Gaussian Bayesian tracking", *Tran. Signal Pr.*, IEEE, **50**(2), 174-188.

Bathe, K.J. and Wilson, E.L. (1987), *Numerical Methods in Finite Element Analysis,* Prentice Hall of India Pvt. Ltd, New Delhi, India.

Chan, T.H.T., Law, S.S., Yung, T.H. and Yuan, X.R. (1999), "An interpretive method for moving force identification", *J. Sound Vib.*, **219**(3), 503-524.

Chan, T.H.T., Yu, L. and Law, S.S. (2000), "Comparative studies on moving force identification from bridge strains in laboratory", *J. Sound Vib.*, **235**(1), 87-104.

Ching, J., Beck, J.L. and Porter, K.A. (2006), "Bayesian state and parameter estimation of uncertain dynamical systems", *Prob. Eng. Mech.*, **21**, 81-96.

Clayton, A. and Peter, R. (1990), "Truck weights as a function of Regulatory limits", *Can. J. Civil Eng.*, **17**, 45-54.

Fryba, L. (1968), *Vibration of Solids and Structures under Moving Loads*, Noordhoff International Publishing, Groningen, Netherlands.

Fryba, L. (1996), *Dynamics of Railway Bridges*, Telford, London.

Green, M.F. and Cebon, D. (1997), "Dynamic interaction between heavy vehicle and highway bridges", *Comput. Struct*., **62**, 253-264.

Hodges, D.H. and Pierce, G.A. (2002), *Introduction to Structural Dynamics and Aero-elasticity*, Cambridge Aerospace Series.

Huang, D.Z. and Wang, T.L. (1992), "Impact analysis of cable stayed bridges", *Comput. Struct*., **43**(5), 897-908.

Inman, D.J. (2001), *Engineering Vibration*, Prentice Hall of India Pvt. Ltd, New Delhi, India.

ISO 8606 (1995), Mechanical vibration-Road surface profiles-reporting measured data.

Kalman, R.E. (1960), "A new approach to linear filtering and prediction method", *J. Basic Eng*., ASME, **191** (82D), 35-45.

Law, S.S., Chan, T.H.T. and Zeng, Q.H. (1997), "Moving force identification: a time domain method", *J. Sound Vib*., **201**(1), 1-22.

Law, S.S., Chan, T.H.T. and Zeng, Q.H. (1999), "Moving force identification: a frequency and time domain analysis"*, J. Dyn. Meas. Contr.*, ASME, 12, 394-401.

Law, S.S. and Fang, Y.L. (2001), "Moving force identification: optimal state estimation approach", *J. Sound Vib*., **239**(2), 233-254.

Law S.S., Bu, J.Q., Zhu, X.Q. and Chan, S.L. (2004), "Vehicle axle loads identification using finite element method", *Eng. Struct*., **26**(8), 1143-1153.

Meirovitch, L. (1967), *Analytical Methods in Dynamics*, Mc. Millan Co., London.

Moses, F (1979), "Weigh-in-motion system using instrumented bridges", *J. Trans Eng*., ASCE, **105**, 233-249.

Nasrellah, H.A. and Manohar, C.S. (2010), "A particle filtering approach for structural system identification in vehicle-structure interaction problems", *J. Sound Vib*., **329**, 1289-1309.

O'Connor, C. and Chan, T.H.T (1988), "Dynamic wheel loads from bridge strains", *J. Struct. Eng*., ASCE, **114**(8), 1703-1723.

Sato, T. and Tanaka, Y. (2013), "Particle relaxation method for structural parameters identification based on Monte Carlo filter", *Smart Struct. Syst*., **11**(1), 53-67.

Shinozuka, M. (1971), "Simulation of multivariate and multidimensional random process", *J. Acoust. Soc. Am*., **49**, 357-367.

Velestos, A.S. and Huang, T. (1970), "Analysis of dynamic response of highway bridges", *J. Eng. Mech*., ASCE, **96**(5), 593-620.

Wen, R.K. (1960), "Dynamic response of beams traversed by two axle loads", *J. Eng. Mech*., ASCE, **86**(5), 91-115.

Yang, Y.B. and Yau, J.D. (1997), "Vehicle-bridge interaction element for dynamic analysis", *J. Struct. Eng*., ASCE, **123**(11), 1512-1518.
Yang, Y.B., Yau, J.D. and Wu, Y.S. (2004), *Vehicle-Bridge Interaction Dynamics*, World Scientific.
Yang, Y.B., Chang, C.H. and Yau, J.D. (1999), "An element for analyzing vehicle-bridge systems considering vehicle's pitching effect", *Int. J. Numer. Meth. Eng*., **46**, 1031-1047.
Yoshida, I. and Akiyama, M. (2013), "Particle filter model updating and reliability estimation of existing structures", *Smart Struct. Syst.*, **11**(1), 103-122.
Yu, L. and Chan, T.H.T. (2007), "Recent research on identification of moving loads on bridges", *J. Sound Vib*., **305**(1-2), 3-21.
Zhu, X.Q. and Law, S.S. (2000), "Study on different beam models in moving force identification", *J. Sound Vib.*, **234**(4), 661-679.

CC